Quantitative Comparison of Solid-State Microwave Detectors

A. M. COWLEY, MEMBER, IEEE, AND H. O. SORENSEN, MEMBER, IEEE

***Abstract*—A method for quantitative comparison of solid-state microwave square-law detectors is presented. The threshold response of the square-law detectors are compared for unit video bandwidth using the concept of Noise Equivalent Power (NEP). NEP is the microwave input power required for unity signal-to-noise ratio in a 1 Hz bandwidth at the output of the detector. Contours of constant NEP in the microwave (RF) and video frequency plane clearly describe the dependence of threshold sensitivity on both video and radio frequencies, and thereby provide comparison of the threshold sensitivities of devices over the entire video and RF frequency spectrum.**

A criterion for the upper RF power limit of square-law operation for detectors is also presented. Dynamic range for a device can be found using this criterion and the threshold sensitivity of the device.

Six solid-state detection devices are described briefly, then compared on the basis of the foregoing concepts. Four of these devices are familiar: the point-contact and planar Schottky-barrier ("hot carrier") diodes, and the tunnel and back diodes. Two relatively new devices are also discussed: the so-called "hot carrier" thermoelectric detector, and the space-charge-limited (SCL) dielectric diode.

SYMBOLS

A = Microwave voltage amplitude, device area
B = Bandwidth
B_0 = Low-frequency susceptance
C = Capacitance
C_B = Barrier capacitance for barrier-type device, i.e., hot carrier, point-contact, tunnel, and back diodes
C_0 = Zero-bias capacitance for barrier-type device
Δi = Incremental direct or low-frequency current which flows in video circuit when microwave signal is applied to nonlinear device
$f(v)$ = Current-voltage function of nonlinear device
$f^{(1)} \cdots f^{(4)}$ = Derivatives of $f(v)$ with respect to v
f_{RF} = Microwave (RF) frequency
f_V = Video frequency
f_c = Cutoff frequency (RF)
f_N = Noise corner
G_0 = Low-frequency conductance
I_0 = Direct bias current in the absence of applied microwave power
i_s = Incremental current in video circuit when microwave power is applied to a detector ($=\Delta i$)
i = Total current through detector
I_s = Saturation current of a hot carrier or point-contact diode
i_N = Noise current in video circuit for 1 Hz video bandwidth
J = Current density
k = Boltzmann's constant
K_N = Noise corner coefficient—amp^{-1} sec^{-1}
$k_1 \cdots k_4$ = Coefficients in current-voltage function for SCL dielectric diode
NEP = Noise Equivalent Power
$(\text{NEP})_0$ = Noise Equivalent Power for $f_{RF} \ll f_c$ and $f_V \gg f_N$
N_c = Effective density-of-states in conduction band of semiconductor
n = Electron density ideality factor
P = Microwave power
P_{RF} = Total RF power absorbed by a device, including parasitic elements
$P_{RF}(\text{USL})$ = Upper square-law limit of P_{RF}
P_B = Microwave power dissipated in nonlinear element of barrier-type device
$P_B(\text{USL})$ = Upper square-law limit of P_B
q = Electronic charge
R_s = Series resistance
R_B = Barrier resistance
R_V = Video resistance
r_0 = Contact radius for TED
TSS = Tangential sensitivity
T = Temperature (degrees Kelvin), electron transit time
t = Noise temperature ratio
t_w = "White noise" temperature ratio
v = Total applied voltage to detector
V_0 = Applied bias voltage
v_N = Noise voltage
W = Thickness (SCLD)
β = Current responsivity—amperes/watt, nonlinear mobility coefficient—cm^2/volt^2
β' = Current responsivity for a device with parasitic series resistance
β_0 = Current responsivity for very small microwave signal
β_0' = Current responsivity for device with series resistance and small microwave signal
γ = voltage responsivity, volts/watt
γ_0 = Low-level voltage responsivity, volts/watt
Δ_1 = Square-law deviation term

Manuscript received May 31, 1966; revised September 8, 1966.
The authors are with -hp- Associates, Palo Alto, Calif.

Δ_2 = Square-law deviation term
Δ = Square-law deviation term = $\Delta_1 - \Delta_2$
ϵ = Dielectric constant
θ = Transit angle = ωT; T = transit time
μ_0 = Low field electron mobility
μ_e = Electron mobility
ρ = Semiconductor resistivity
τ_d = Dielectric relaxation time = $\rho\epsilon$
τ_E = Energy relaxation time
τ_p = Momentum relaxation time
ω = Radian frequency

IN THIS PAPER, a method for quantitative comparison of solid-state microwave square-law detectors is presented. Six basic device classes are considered in the comparison: hot carrier (Schottky barrier) diodes, point-contact diodes, thermoelectric detectors, tunnel diodes, backward tunnel diodes, and space-charge-limited (SCL) dielectric diodes. The bases chosen for comparison are threshold sensitivity, frequency response, and dynamic range of square-law operation. The paper is essentially a survey of what the authors feel to be devices of current or potential importance as detectors.

In order to compare the devices on an equal basis, the assumption will be made that, with appropriate tuning, each device can be matched to the RF power source. This is equivalent to the assumption that all of the *available* microwave power is absorbed by the device.

I. Threshold Sensitivity

We will express threshold sensitivity of each device in terms of the Noise Equivalent Power (NEP) which is defined as the RF input power required to produce an output signal-to-noise ratio of unity, for a bandwidth of one hertz. By using this definition, we obtain a measure of threshold sensitivity characteristic of the device itself, completely independent of any associated video amplification circuitry. With the present-day availability of extremely low noise video amplifiers, this seems to be a reasonable procedure, since it is now practical to measure detector sensitivity in circuits where amplifier noise may be essentially ignored. The assumption of unit bandwidth is not a limitation, but rather a very useful concept for examining devices operating at video frequencies in the $1/f$ noise region. A common practice among manufacturers of microwave detector diodes is to specify diode performance for a large video bandwidth, often larger than 10 MHz. This practice makes comparison impossible for devices operating at low video frequencies.

For a square-law detector, the commonly used Tangential Sensitivity (TSS) is related to NEP by

$$\mathrm{TSS} = 2.5(\mathrm{NEP})\sqrt{B} \tag{1}$$

where B is the video bandwidth. Equation (1) expressed in dB becomes

$$\mathrm{TSS_{dB}} = \mathrm{NEP_{dB}} + 4 + 5 \log_{10} B. \tag{2}$$

The tangential sensitivity thus bears a simple fixed relationship to NEP for a known bandwidth, and either quantity completely specifies the threshold performance of a detector.

II. Nonlinear Device Analysis

All of the devices considered here depend for their detection properties on a nonlinear current-voltage characteristic. It is therefore useful to briefly review the analysis of a nonlinear device operated as a low-level detector. The current-voltage function of a nonlinear device can be denoted by

$$i = f(v). \tag{3}$$

Microwave detectors are often operated with a dc bias; therefore, for generality, we will write the voltage v as the superposition of a dc bias voltage V_0 and a microwave input voltage $A \cos \omega t$

$$v = V_0 + A \cos \omega t. \tag{4}$$

Expanding (3) in a power series about V_0, and substituting (4), we obtain the fundamental and dc terms as follows:

$$i - I_0 = \left[\frac{A^2}{4} f^{(2)} + \frac{A^4}{64} f^{(4)}\right] + \left[A f^{(1)} + \frac{A^3}{8} f^{(3)}\right] \cos \omega t \tag{5}$$

where $f^{(1)}, \cdots, f^{(4)}$ are derivatives of $f(v)$ with respect to v, evaluated at V_0, and I_0 is $f(V_0)$.

The average microwave power P absorbed by the device can be found by multiplying (5) by the input voltage $A \cos \omega t$ and integrating over one microwave period. This leads to the following expression for P:

$$P = \frac{A^2}{2}\left[f^{(1)} + \frac{A^2}{8} f^{(3)}\right] \tag{6}$$

which is evident almost by inspection. The first bracketed term on the right-hand side of (5) is the detected current Δi, the time average incremental increase in current due to the application of microwave power. The ratio of Δi to P is called the current responsivity β, and can be written in the form

$$\frac{\Delta i}{P} = \beta = \beta_0 \left[\frac{1 + \Delta_1}{1 + \Delta_2}\right] \tag{7}$$

where

$$\beta_0 = \frac{1}{2} \frac{f^{(2)}}{f^{(1)}} \tag{8}$$

and

$$\Delta_1 = \frac{A^2}{16} \frac{f^{(4)}}{f^{(2)}} \tag{9}$$

$$\Delta_2 = \frac{A^2}{8} \frac{f^{(3)}}{f^{(1)}}. \tag{10}$$

Using (6), and making suitable approximations, (7) can be written

$$\beta \simeq \beta_0[1 + \Delta_1 - \Delta_2] = \beta_0[1 + \Delta] \tag{11}$$

where

$$\Delta = \frac{1}{8}\frac{P}{f^{(1)}}\left[\frac{f^{(4)}}{f^{(2)}} - 2\frac{f^{(3)}}{f^{(1)}}\right]. \tag{12}$$

The quantity β_0 is the low-level current responsivity of the device. The quantity Δ shows how, for higher power levels, the detector response deviates from true square-law operation. The upper limit of square-law operation, $P(\text{USL})$, is defined as that microwave input power which produces a maximum prescribed deviation from square-law operation. For reasons which will be stated below, we set this maximum deviation at 0.3 dB; that is, we wish to satisfy

$$10 \log_{10} (1 + |\Delta|) = 0.3 \text{ dB}. \tag{13}$$

Using (12), this leads to

$$P(\text{USL}) = \frac{0.56 f^{(1)}}{\left|\frac{f^{(4)}}{f^{(2)}} - 2\frac{f^{(3)}}{f^{(1)}}\right|}. \tag{14}$$

In a paper dealing with dynamic range of crystal (point-contact) detectors, Sorger and Weinschel [1] choose 0.1 dB rather arbitrarily as a maximum deviation. The reason for our choice of 0.3 dB is as follows: the commonly accepted lower power limit of a device when operated as a detector is the tangential sensitivity TSS. When the input power level is equal to TSS, the detector output, as measured, for example, by an rms ammeter or voltmeter, is given by

$$(\Delta i)^2_{\text{total}} = (\Delta i)^2_{\text{signal}} + (\Delta i)^2_{\text{noise}}. \tag{15}$$

But since input power is equal to TSS, we know that $(\Delta i)_{\text{signal}} = 2.5(\Delta i)_{\text{noise}}$ and the *error* in measuring power, expressed in dB, is given by

$$10 \log_{10}\left(\frac{(\Delta i)^2_{\text{total}}}{(\Delta i)^2_{\text{signal}}}\right)^{1/2} = 10 \log_{10}\left(1 + \left(\frac{1}{2.5}\right)^2\right)^{1/2} = 0.3 \text{ dB}. \tag{16}$$

A comparison of (13) and (16) shows that our definitions for upper and lower limits of square-law operation result in equal error.

III. Description of Devices; NEP Contours

A brief description of the electrical characteristics of the solid-state detection devices to be considered in this paper is now in order. We will begin by describing the electrical characteristics of hot carrier diodes and point-contact diodes, since the two are similar in their physical theory of operation. A useful comparison technique, the NEP contour method, is also introduced in this section.

A. Hot Carrier and Point-Contact Diodes

Hot carrier (planar Schottky barrier) and point-contact diodes are metal-semiconductor devices which are described by the Schottky theory of rectification at a metal-semiconductor contact [2]. The chief difference between the two is their construction; the point-contact diode is fabricated by pressing a fine metal point into the surface of the semiconductor, followed sometimes by an electrical or mechanical forming operation. Hot carrier diodes are fabricated by depositing a metal film on the prepared surface of the semiconductor. Some obvious advantages of the latter method are closer control of geometry and better resistance to mechanical shock. It is difficult, however, to make hot carrier diodes with capacitance as small as that of a point-contact diode.

Hot carrier and point-contact diodes depend on majority carrier conduction, in contrast to the minority carrier operation of ordinary p-n junction diodes. Since there are no minority carrier storage effects, these devices are potentially capable of operation up to frequencies approaching the reciprocal of the dielectric relaxation time τ_d of the semiconductor crystal. For practical devices this frequency will be of the order of 1000 GHz. However, other considerations, particularly series resistance and junction capacitance, will be more important in the determination of frequency response for practical hot carrier and point-contact diodes, placing their upper frequency limit at lower values.

Hot carrier and point-contact diodes are described electrically by the equivalent circuit shown in Fig. 1, and by the $v-i$ relationship

$$i = I_s\left[\exp\left(\frac{q}{nkT}v\right) - 1\right] \tag{17}$$

where n is a number somewhat greater than unity for point-contact diodes, and very nearly unity for hot carrier diodes.

Referring to Fig. 1, the elements R_B and C_B are, respectively, the incremental resistance and capacitance associated with the junction, or barrier, region of the device, while R_s is a parasitic series resistance associated with the bulk semiconductor substrate and any contact

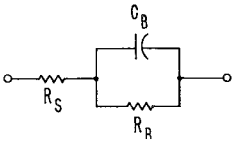

R_S – PARASITIC SERIES RESISTANCE
R_B – BARRIER RESISTANCE
C_B – BARRIER CAPACITANCE

Fig. 1. RF equivalent circuit of barrier-type devices: hot carrier, point-contact, tunnel, and back diodes.

resistance arising from soldered connections, whisker, etc. Equation (17) is the static, or dc, characteristic of the junction, not including series resistance R_s. The current I_s is called the saturation current, and depends on the junction area, and the metal and semiconductor used to form the junction. The dynamic resistance associated with the barrier is obtained from (17) as

$$R_B = \frac{nkT}{q(I_0 + I_s)} \tag{18}$$

where I_0 is the direct bias current.

For a diode fabricated from a semiconductor with uniform impurity density, the capacitance C_B can be expressed as

$$C_B = \frac{C_0}{\left(1 + \frac{V_0}{V_B}\right)^{1/2}} \tag{19}$$

where C_0 is the zero-bias junction capacitance and V_B is a parameter having the dimensions of volts, known as the diffusion potential; V_B depends on the metal and upon the semiconductor impurity density.

Before applying the theory of Section II to the hot carrier or point-contact diode, we must take into account the fact that not all of the microwave power absorbed in the device is absorbed in the nonlinear portion of the device, i.e., the nonlinear resistance R_B. A portion of the power is dissipated in the parasitic series resistance R_s. A simple analysis of the equivalent circuit of Fig. 1 yields the following relation for the ratio of the power absorbed in R_B, to the *total absorbed power* P_{RF}:

$$\frac{P_B}{P_{RF}} = \frac{1}{\left[1 + \frac{R_s}{R_B}\right][1 + (f/f_c)^2]} \tag{20}$$

where

$$f_c = \frac{\left[1 + \frac{R_s}{R_B}\right]^{1/2}}{2\pi C_B (R_s R_B)^{1/2}}. \tag{21}$$

We can now use the theory of Section II with the understanding that power P, as used in that section, refers to the power P_B for the point-contact or hot carrier diode. Equation (20) is used when a detector parameter must be referred to total microwave input power.

The ratio of Δi to P_B, as obtained using (8), (11), (12), and (17) is

$$\frac{\Delta i}{P_B} = \frac{q}{2nkT}\left[1 - \frac{1}{8}\,\frac{q}{nkT(I_0 + I_s)}\,P_B\right]. \tag{22}$$

The ratio $\Delta i/P_B$ will be denoted by β, as in the preceding section. However, the quantity of interest to the microwave engineer is the ratio $\Delta i/P_{RF}$, which may be obtained by multiplying β by the ratio given in (20). The result will be denoted by β'. Referring to (20) and (22), the *low-level* current responsivity for the device becomes

$$\beta_0' = \frac{q}{2nkT}\,\frac{1}{\left[1 + \frac{R_s}{R_B}\right][1 + (f/f_c)^2]}. \tag{23}$$

Note that the frequency dependence for β_0' is contained entirely in the last bracketed term in the denominator.

Using (13) and (22), one obtains the upper square-law limit of P_B as

$$P_B(\mathrm{USL}) = (0.56)\,\frac{nkT}{q}\,(I_0 + I_s). \tag{24}$$

Using (20), the upper square-law limit for total microwave power input to the device is

$$P_{RF}(\mathrm{USL}) = 0.56\left[\frac{nkT}{q}\right](I_0 + I_s)\left[1 + \frac{R_s}{R_B}\right] \cdot [1 + (f/f_c)^2]. \tag{25}$$

In order to calculate threshold sensitivity of either the point-contact or the hot carrier diode, the noise properties of the device must be known. Both devices exhibit $1/f$ noise, in addition to a uniform spectrum of "white noise" [3]–[6]. The noise of either device can be characterized in terms of its *noise temperature ratio t*. Referring to the video equivalent circuit for the diode shown in Fig. 2, the device has associated with its video resistance a noise current source i_N. (The video resistance R_V is simply $R_B + R_s$, the sum of series and barrier resistance.) A resistor of value R_V would have a current source $i_N^2 = 4kTB/R_V$ associated with it. The diode exhibits excess noise characterized by the noise temperature ratio t, so the corresponding current source (squared) for the diode is $4kTBt/R_V$. As discussed earlier, the video bandwidth B for the present work is taken to be unity.

Again referring to Fig. 2, the incremental detected current corresponding to a given input power P_{RF} is simply

$$i_s = \Delta i = \beta_0' P_{RF}. \tag{26}$$

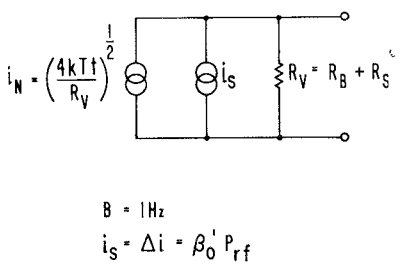

Fig. 2. Video equivalent circuit for barrier-type devices.

The noise current in the device is

$$i_N = \left[\frac{4kTt}{R_V}\right]^{1/2} \tag{27}$$

for unit video bandwidth.

The noise equivalent power (NEP) is that input power which results in equal output signal and noise power, or equivalently, equal signal and noise current at the output. Hence, using (26) and (27)

$$\text{NEP} = \frac{i_N}{\beta_0'}. \tag{28}$$

A device with $1/f$ noise has a noise temperature ratio given by the expression

$$t = t_w\left(1 + \frac{f_N}{f_V}\right) \tag{29}$$

where f_N is the familiar "noise corner," f_V the video frequency, and t_w the "white-noise" temperature ratio; t_w is usually less than unity [7].

Using (23), (27), (28), and (29), we obtain after some manipulation:

$$\text{NEP} = \frac{2nkT}{q}\left[\frac{4kTt_w}{R_B}\right]^{1/2}\left[1 + \frac{R_s}{R_B}\right]^{1/2} \cdot \left[1 + \left(\frac{f}{f_c}\right)^2\right]\left[1 + \frac{f_N}{f_V}\right]^{1/2}. \tag{30}$$

The last two bracketed terms in (30) depend on RF and video frequency, respectively. The remainder of the expression is frequency independent. If the frequency independent part of (30) is denoted by $(\text{NEP})_0$, then the expression can be rewritten

$$\text{NEP} = (\text{NEP})_0\left[1 + \left(\frac{f}{f_c}\right)\right]^2\left[1 + \frac{f_N}{f_V}\right]^{1/2}. \tag{31}$$

Note that this expression is general, and applies to any device whose equivalent circuits are of the forms given in Figs. 1 and 2, and which has $1/f$ noise. Examples of devices whose threshold performance can be described by (31) are the backward diode and the tunnel diode, in addition, of course, to the hot carrier and point-contact diodes.

In the course of studies conducted at the authors' laboratory [8], it has been found that the noise corner f_N of hot carrier and point-contact diodes fits an equation of the form

$$f_N = K_N I_0. \tag{32}$$

The constant K_N varies widely depending on the diode type. It is typically much smaller for hot carrier diodes than for point-contact diodes, indicating superior $1/f$ noise characteristics for the hot carrier diode. Figure 3 shows a plot of some of the data obtained during this study.

Equations (30) and (31) are particularly convenient for the analysis of hot carrier and point-contact diodes, because given the v-i characteristic for the device, and the value of K_N, all other quantities, i.e., R_B, C_B, f_N, and f_c, may be calculated for any value of bias current I_0, and (30) or (31) can be used to calculate NEP. TSS for unit bandwidth is obtained by simply adding 4 dB to NEP, and $P_{RF}(\text{USL})$ can be found from (25). The dynamic range is the difference between TSS and $P_{RF}(\text{USL})$, expressed in dB.

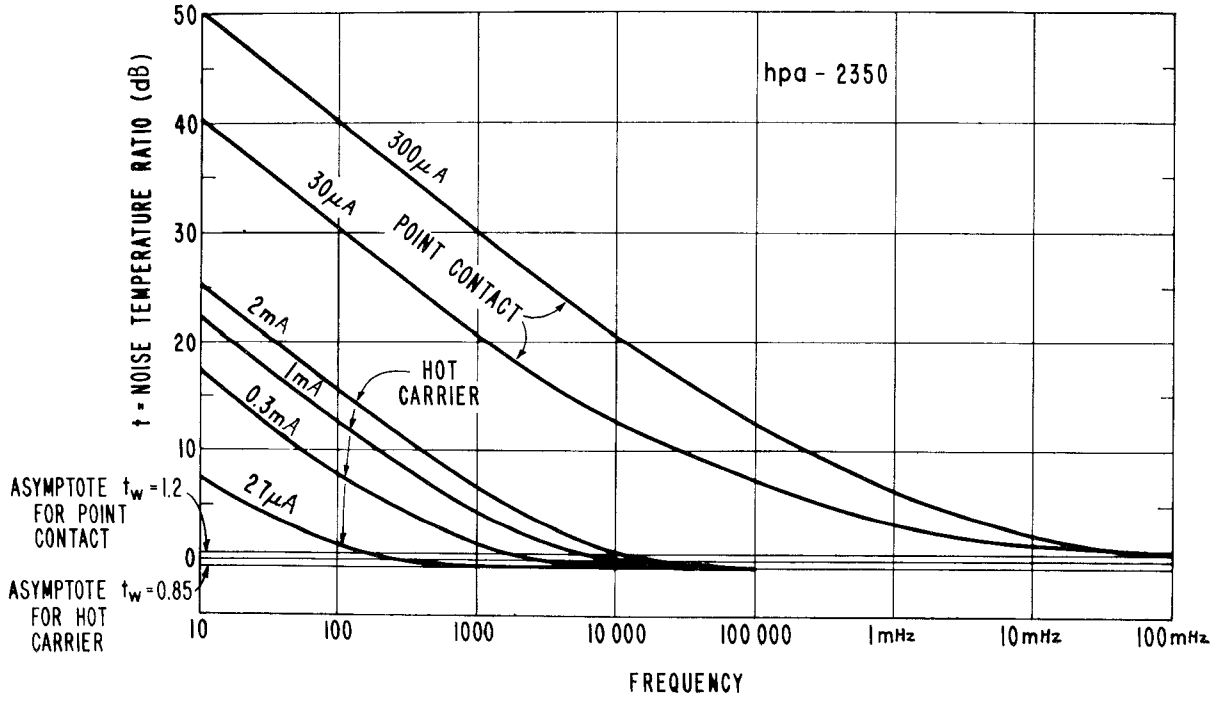

Fig. 3. Noise characteristics of hot carrier and point-contact diodes.

B. NEP Contours

The current responsivity β_0' for a detector is, in general, a function of the microwave frequency f_{RF}, as exemplified by (23) for the hot carrier and point-contact diodes. This functional dependence may not be expressed analytically, but in practice it can always be obtained by experiment as a graph of β_0' vs. f_{RF}. Similarly, for a detector with excess noise, the noise current i_V in the video circuit is a function of video frequency f_V; i_N is defined in this paper as the noise current for a video bandwidth of one hertz. Using (28), NEP is therefore a function of both f_{RF} and f_V; that is

$$\text{NEP} = \text{NEP}(f_{RF}, f_V) \tag{33}$$

in functional notation. Equation (33), for a fixed value of NEP, generates a curve in the RF-video frequency plane. Such a curve will be defined as an *NEP contour*. By picking several values of NEP, a family of NEP contours can be obtained, and these contours completely specify the threshold performance of a detector. Given the functions $\beta_0'(f_{RF})$ and $i_N(f_V)$, as measured experimentally or derived analytically, NEP contours can be constructed, very straightforwardly, using (28).

If NEP contours for two devices are plotted on the same graph, the points of intersection of contours of *equal* NEP generate a line in the RF-video frequency plane. This line divides the plane into regions of superior threshold sensitivity for each of the two devices. To illustrate this principle, (31) has been used to construct NEP contours for two familiar devices, a hot carrier diode, and a point-contact diode. The values for $(\text{NEP})_0$, f_N and f_c were calculated from data typical of two such diodes, using (18), (19), (21), (30), and the noise data shown in Fig. 3. The contours are shown in Fig. 4. In the lower left-hand region, the hot carrier diode has superior threshold sensitivity to the point-contact diode. In the upper right-hand region, the point-contact diode is superior. Figure 5 shows these two "preference regions" clearly. The diodes chosen for comparison were each assumed to be biased with 50 μA of forward current. It is worthwhile emphasizing the fact that, while the point-contact diode is clearly superior in the higher RF and video frequency region, the hot carrier diode is superior at lower video frequencies. For example, in a 1 kHz video frequency application, the hot carrier diode is superior up to radio frequencies in excess of 10 GHz. This is indeed surprising, since an L-band hot carrier diode was chosen for the comparison. The reason for this result is quite evident, however; despite its poorer high-frequency response, the superior $1/f$ noise performance, i.e., lower noise corner, of the hot carrier diode enables it to perform better than the point-contact diode at lower video frequencies.

It is interesting to compare the dynamic range of square-law response for the two diodes compared in Figs. 4 and 5. The values of n for point-contact and hot carrier diodes, respectively, are typically 1.5 and 1.05. A conservative value of R_s for either diode is 20 ohms. The white noise temperature t_w is typically somewhat smaller than unity, but will be taken as unity for these calculations. For these parameter values, the dynamic range of both devices is about 59.5 dB. For the same bias conditions, $(\text{NEP})_0$ as calculated for the diodes from (30), (assuming $f \ll f_c$ and $f_V \gg f_N$) is -93.5 dBm for the point-contact diode and -95 dBm for the hot carrier diode. Table I contains this data and data calculated for the other devices.

Hot carrier and point-contact diodes are very conveniently compared by the method presented in this section. One only needs to know R_s, R_B, C_B, n, and f_N, in order to compare performance of the devices over the entire RF-video frequency plane. These parameters are relatively easy to measure or calculate; if the noise corner parameter K_N is once found, the noise corner can be calculated for any bias current, eliminating the necessity for measuring f_N for each bias current. In general, it is observed for hot carrier diodes that (18) and (19) are obeyed very closely, with $n \simeq 1.0$ for (18). A simple measurement of C_0 and V_B allows C_B to be calculated via (19). Figure 6 shows C_B and R_B vs. bias for a typical hot carrier diode, showing near perfect agreement with (18) and (19).

C. Tunnel and Back Diodes

The tunnel and back diodes depend for their interesting current-voltage behavior upon the phenomenon of quantum-mechanical tunneling [9]. They are essentially p-n junctions whose impurity density is made purposely high in order to produce a very narrow p-n junction across which electrons can tunnel easily. Tunneling current occurs at much lower values of applied voltage than ordinary p-n junction current, increasing as forward voltage is increased, then decreasing again. When operated as detectors, tunnel diodes are ordinarily biased in the forward direction at a voltage somewhat lower than the voltage corresponding to the peak tunnel current I_p [10]. However, at least one author reports the preliminary results of using a tunnel diode biased into the negative resistance region as a video detector [11]; due to the scarcity of experimental data for this mode of operation, it will not be discussed further in this paper.

Back diodes are simply tunnel diodes which are designed for a lower peak current than the usual tunnel diode. They are called "back" diodes because they are usually operated on the reverse portion of the i-v characteristic [12]. They typically have higher values of origin resistance than tunnel diodes, due to their lower peak current.

The RF equivalent circuit for a tunnel or back diode is essentially the same as that for the hot carrier and point-contact diodes; the diodes have a series resistance due to the bulk semiconductor and contacts, and a parallel combination of incremental junction conductance and capacitance. Tunneling is a majority carrier

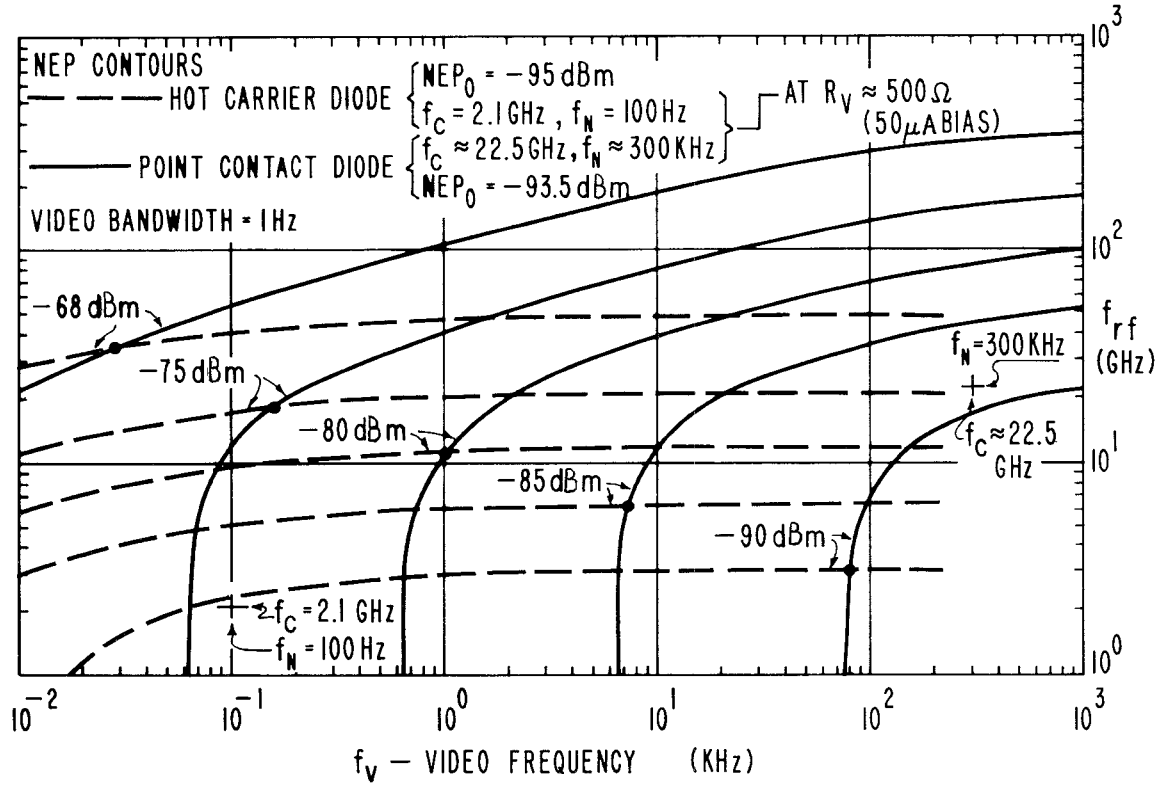

Fig. 4. NEP plots for hot carrier and point-contact diodes

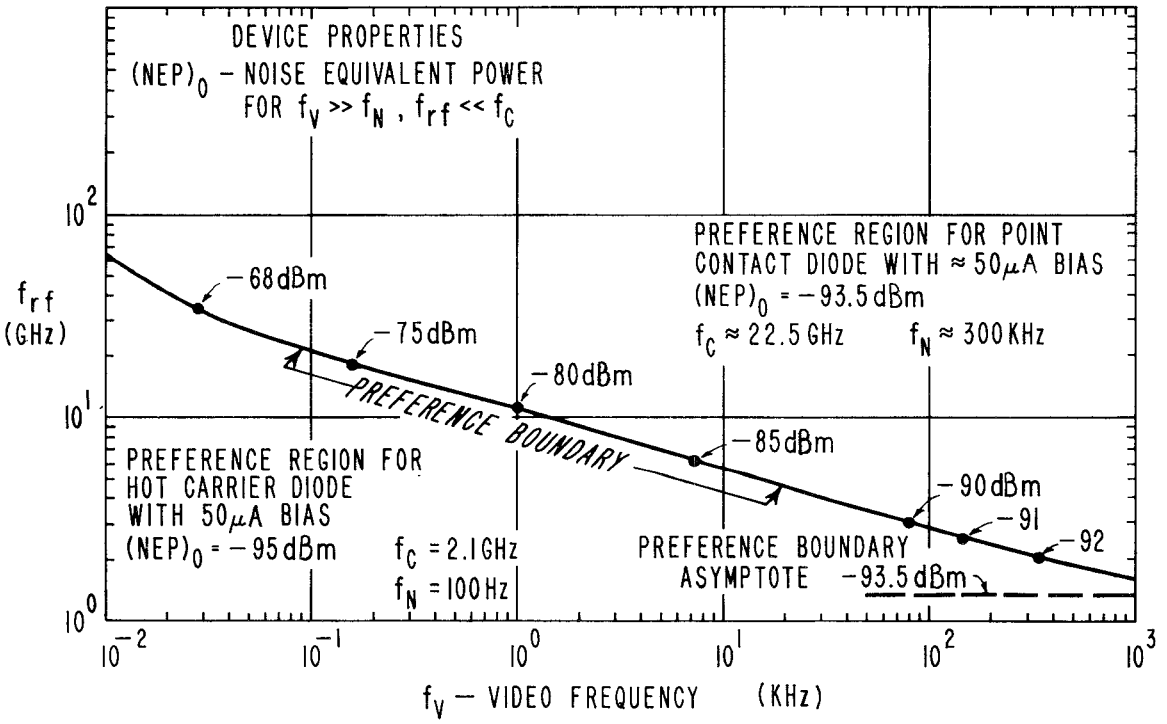

Fig. 5. "Preference" regions for hot carrier and point-contact diodes whose NEP plots are shown in Fig. 4.

TABLE I

COMPARISON OF TYPICAL DEVICES

Device	Bias (μA)	$R_B(\Omega)$	$R_s(\Omega)$	C_B(pF)	f_c(GHz)	f_N(kHz)	(1) β_0 volt^{-1}	(NEP) dBm°	(2) P(USL) dBm	Dyn. (3) Range dB
"Low Noise"										
PC Diode	$\simeq$50	$\simeq$500	20	$\simeq$0.10	20	300	$\gtrsim$ 13	−93.5	−30	59.5
PC Diode	5–600	$\gtrsim$ 30	20	$\gtrsim$0.20	30	>5000	$\gtrsim$ 8	−87	−18	65
HC Diode	50	500	20	1.2	1.2	0.1–0.2	19	−95	−31.5	59.5
HC Diode	5–600	30	20	1.4	5.8	1.5	12	−88.5	−19.5	65
HC Diode	50	500	10	0.9	5.8	0.2	19.5	−95.5	−31.5	60
HC Diode	5–600	40	10	1.1	8.1	2.0	16	−90	−21.0	65
HC Diode	50	500	5	0.9	8.2	0.2	20	−95.5	−31.5	60
HC Diode	5–600	45	5	1.1	10.7	2.0	18	−90.5	−21.5	65
Back Diode	0	90	10	1.0	5.5		25	−93	−35.5	53.5
Tunnel Diode	1 mA	45	5	1.0	11.2	50	100	−97.5	−43.5	50
Tunnel Diode	?	45	5	1.0	11.2	10–50	100	−97.5	−43.5	50
Thermoelectric Detector	—	$R_V=100\ \Omega$		—	∞	0	0.003	−54	+ 4.5	54.5
Thermoelectric Detector	—	$R_V=500\ \Omega$		—	∞	0	0.006	−60.5	−2	54.5
Thermoelectric Detector	—	$R_V=1000\ \Omega$		—	∞	0	0.007	−62.5	−5	53.5
Thermoelectric Detector	—	$R_V=5000\ \Omega$		—	∞	0	0.009	−67.0	−12	51
SCLD	0.5v	$R_V=500\ \Omega$		1.0 pF	—	?	1.0	−82.5	−6	72.5
SCLD	2.0v	$R_V=2000\ \Omega$		1.0 pF	—	?	0.2	−70.0	−11	55.5

1) Overall current responsivity for $f \ll f_c$.
2) $f \ll f_c$.
3) $f_V \gg f_N$.

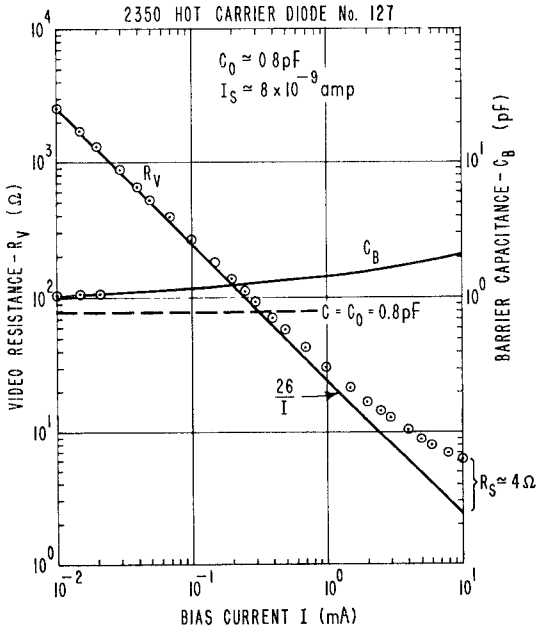

Fig. 6. Barrier resistance and capacitance vs. bias for typical hot carrier diode.

phenomenon; the tunnel and back diode characteristics are therefore subject to basically the same frequency limitations as hot carrier and point-contact diodes. In fact, tunnel and back diodes may be analyzed in precisely the same way as the hot carrier and point-contact diodes, if the quantities R_s, R_B, C_B, f_N, and β_0, are known for the operating point in question.

A convenient analytic expression for the current voltage function is not available for the tunnel and back diodes as it is for the hot carrier and point-contact devices. Theoretical tunneling characteristics have been computed numerically [13], [14]; these are in reasonable agreement with experiment, but are not readily useable in the design and analysis of the devices in microwave applications.

Recent publications [15], [16], as well as many manufacturers' specification sheets, indicate that the current responsivity of tunnel and back diodes can be of the order of 30 volts^{-1} at zero and moderate forward or reverse bias. By biasing the tunnel diode near its peak current, enormous current sensitivities can be obtained; however, this increase is accompanied by a serious loss of dynamic range and the onset of instability and $1/f$ noise.

Dynamic resistance of the tunnel devices is usually very low, often of the order of 10 Ω. Back diodes can be made to have 50 Ω total resistance at zero or moderate forward bias, while a tunnel diode must often be biased near the peak current to obtain a match to 50 Ω transmission line. Series resistance R_s can be as low as 5 Ω for the tunnel diode. Capacitance of the diodes is typically high compared to point-contact diodes, mainly due to the narrow junction width. Capacitance of commercial back and tunnel diodes is usually greater than 0.5 pF. However, Burrus [12] has reported capacitances less than 0.1 pF for special experimental point-contact tunnel diodes used as detectors.

Noise in tunnel and back diodes has been studied by a number of authors [15], [17], [18]. Yajima and Esaki [17] measured $1/f$ noise in germanium tunnel diodes; one of their observations was that $1/f$ noise seems to be related in some way to the diode "excess" current, a current which occurs in the forward direction after the tunnel current peak and before the onset of p-n junction current; it is thought that the excess current is due to the presence of defect levels in the forbidden gap of the narrow p-n junction. Follmer [18] deduced the noise temperature ratio t for back diodes, and found, in general agreement with Yajima and Esaki, that the back diode has extremely low $1/f$ noise for moderate bias levels, with typical noise corners less than 1 kHz. Eng [15] presents data for the $1/f$ noise in biased back diodes, and while his data indicates somewhat higher $1/f$ noise than that of Follmer, the noise for his back diodes is still 10 to 15 dB less than for a so-called low-noise Doppler mixer point-contact diode. Finally, we have ourselves measured $1/f$ noise for a small number of back and tunnel diodes, and find noise corners of the order 1 kHz for moderate ($\simeq$100 μA) bias levels for back and tunnel diodes, but considerably higher values, of the order of 10 kHz and above, for devices biased near the peak current. Table II presents a compilation of data measured in the authors' laboratory and taken from the literature.

TABLE II
NOISE CORNER FOR TUNNEL AND BACK DIODES

Device	Bias Condition	Source	f_N
Back Diode	50–100 μA	Eng [15]	30–50 kHz
Back Diode	——	Follmer [18]	<1 kHz
Back Diode	100 μA	Authors' meas't	<1 kHz
Tunnel Diode	1 mA	Authors' meas't	50 kHz

Let us compare the performance of a 100 Ω unbiased back diode, and a tunnel diode biased near the peak current, using the data of Chase and Chang [10]. For the unbiased back diode, cutoff frequency, $(\mathrm{NEP})_0$ and noise corner are 5.5 GHz, −93.5 dBm, and zero, respectively. For the tunnel diode biased near I_{peak}, the corresponding quantities are 11 GHz, −97.5 dBm, and approximately 50 kHz. The noise corner is an estimate based on Table II. This data, together with similar data for the other detectors, is summarized in Table I.

Dynamic range for the tunnel and back diodes is difficult to predict, theoretically, without an analytical expression for the current-voltage function. In general, dynamic range for these devices is best when the video amplifier presents a very high impedance to the detector, i.e., when the detector operates into an open circuit. Dynamic range gets poorer as the diodes are biased nearer to the peak current. As a *crude estimate* of the dynamic range, let us first observe that (22) may be written

$$\beta = \beta_0[1 - \tfrac{1}{2}\beta_0^2 R_B P_B] \tag{34}$$

for the hot carrier and point-contact diodes, where we have used (18). We find the square-law deviation term Δ from (34) as

$$\begin{aligned}\Delta &= -\tfrac{1}{2}\beta_0^2 R_B P_B \\ &= -\tfrac{1}{2}\beta_0^2 R_B P_{\mathrm{RF}} \Big/ \left(1 + \frac{R_s}{R_B}\right)\end{aligned} \tag{35}$$

if we consider microwave frequencies less than f_c. From (35) we can write $P_{\mathrm{RF}}(\mathrm{USL})$ as

$$P_{\mathrm{RF}}(\mathrm{USL}) = \frac{0.14}{\beta_0^2 R_B}\left(1 + \frac{R_s}{R_B}\right) \tag{36}$$

using the criterion (13). If we now assume that (36) holds for the tunnel devices as well as for the hot carrier and point-contact diodes, we can estimate the dynamic range for the devices from knowledge of R_B, R_s, and β_0. Use of (36) for the tunnel devices is equivalent to assuming that the ratios of the derivatives of the i-v function used in (12) are the same for the tunnel devices as they are for the point-contact and hot carrier diodes.

This probably results in an overestimation of the dynamic range, particularly in the case of the tunnel diode biased near the peak current; the device is particularly sensitive to self-biasing by the microwave signal in this region of operation, with a consequent change in video resistance.

D. Thermoelectric Detector

The thermoelectric detector depends for its detection properties upon the thermoelectric effect for "hot" majority carriers in a semiconductor. The carriers are "heated" by the microwave RF field, and the lattice temperature remains relatively unchanged. Referring to Fig. 7, the device can be readily analyzed in the hemispherical geometry shown. Harrison and Zucker [19] have performed an approximate analysis, and present a detailed discussion of the device. We have performed an analysis which takes into account the effect of nonlinear mobility in the semiconductor and will present the results in this section. Nonlinear mobility imposes an upper limit on square-law operation of this device.

The thermoelectric detector is an ohmic device as seen by the video circuit, and is operated without bias. Its video resistance can be calculated from standard spreading resistance formulas. In actual practice, the smaller contact is often nearly flat, or planar, and for a planar circular contact of radius r_0, the video resistance is given by

$$R_v = \rho/4r_0 \tag{37}$$

where ρ is resistivity of the semiconductor.

The hemispherical geometry has been chosen for convenience in deriving the responsivity of the device, and provides a result which is in reasonable conformity with experiment. The expression which is derived for γ, the open circuit voltage responsivity in volts per watt is,

$$\gamma = \frac{\tau_E}{3\pi q n r_0^3}\left[\frac{3}{2} + \ln\frac{N_c}{n}\right]\left[1 + 0.8\beta\frac{P_{RF}}{nq\mu_0\pi^2 r_0^3}\right] \tag{38}$$

$$= \gamma_0(1 + \Delta) \tag{39}$$

where

$$\gamma_0 = \frac{\tau_E}{3\pi q n r_0^3}\left[\frac{3}{2} + \ln\frac{N_c}{n}\right] \tag{40}$$

$$\Delta = 0.8\beta\left[\frac{P_{RF}}{nq\mu_0\pi^2 r_0^3}\right] \tag{41}$$

τ_E = energy relaxation time for "hot" carriers
r_0 = small contact radius
n = carrier concentration in semiconductor
N_c = density of electronic states in conduction band of semiconductor
β = nonlinear mobility coefficient
μ_0 = low field mobility in semiconductor
P_{RF} = absorbed microwave power
q = electronic charge.

The open circuit voltage developed for unit absorbed power is a constant for low power levels, but deviates from a constant as larger powers are absorbed. The deviation is positive according to (41). This behavior has been observed experimentally in devices constructed in -hp- Laboratories,[1] and is shown for a typical device in Fig. 8.

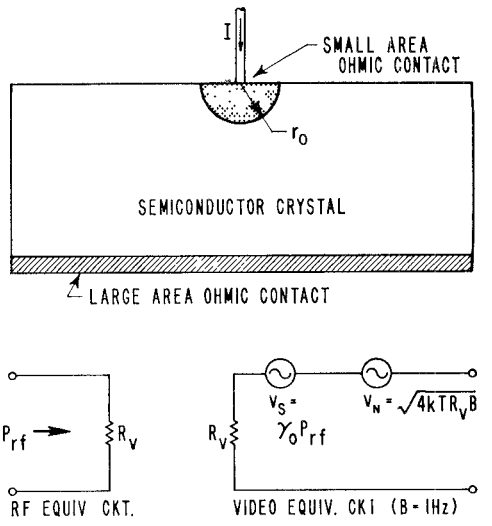

Fig. 7. Thermoelectric detector.

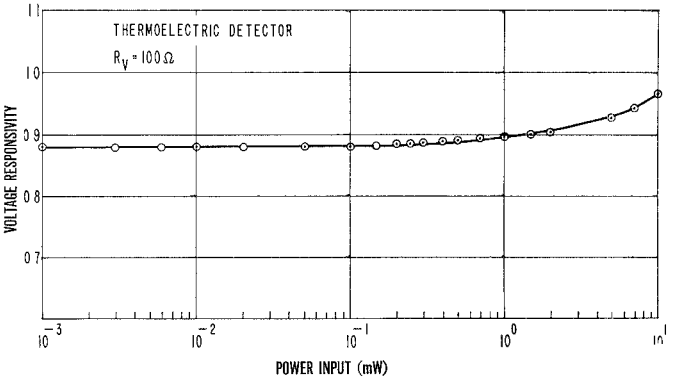

Fig. 8. Voltage responsivity of thermoelectric detector vs. applied RF power.

Qualitatively, the operation of the TED is simple; high electric field strength at the small contact causes localized electrical heating of electrons. These more energetic electrons tend to move away from the contact into the bulk silicon, the small contact thereby becoming positive.

The upper frequency limit of operation of the thermoelectric detector is set by the relaxation time for hot carriers. Generally speaking, the response of carriers to the microwave signal will begin to decrease as the frequency approaches the reciprocal of the momentum relaxation time, about 1000 GHz in the case of silicon, with $\tau_p \simeq 10^{-13}$ seconds. Thus, for practical purposes, the thermoelectric detector when used as a microwave detector has virtually no upper frequency limit.

[1] This data was kindly furnished by L. Wright of -hp- Labs., Palo Alto, Calif.

Noise considerations for the TED are also very simple; the device has the noise properties of a resistor whose value is R_V, the video resistance. Thus, the "noise corner" is essentially zero, i.e., there is no $1/f$ noise. This result has been verified in our laboratories.

The thermoelectric detector appears as a simple resistor to the microwave circuit; its microwave impedance is equal to its video impedance, i.e., the spreading resistance of the contact. The impedance of the device may be controlled only by changing the geometry; for a given resistivity semiconductor, a smaller contact yields a device with higher resistance. Voltage sensitivity γ also increases as the contact is made smaller for a given resistivity. If contact radius is fixed, increasing the resistivity increases both resistance and sensitivity. There is an upper practical limit to the resistance one desires for a detector, and that is the maximum resistance that can be matched to the microwave transmission line. If we fix the resistance at some value, by (37) we have fixed the quantity ρ/r_0. Resistivity ρ is approximately inversely proportional to carrier density n, so from (40) the voltage sensitivity is proportional to $1/r_0^2$. For a desired value of resistance for the device, the sensitivity can be maximized by making the contact radius as small as possible. Extremely small contact size has been obtained in some commercial units by using a point contact, presumably plated and formed by heating or passing current through it. This technique has the usual disadvantages associated with point contacts, primarily lack of resistance to mechanical shock, and lack of uniformity in performance parameters from unit to unit. Planar techniques can also be used to fabricate thermoelectric detectors; the limiting factor here is the size of the contact. It is practical with present technology to make planar contacts a few microns in diameter.

Let us make some estimates of the sensitivity of a practical thermoelectric detector. For silicon, we have

$$\beta \simeq 5 \times 10^{-8} \frac{\text{cm}^2}{\text{volt}^2}, \qquad \mu_0 = 1350 \text{ cm}^2/\text{volt-sec},$$

$$N_c \simeq 3 \times 10^{19} \text{ cm}^{-3}.$$

On the basis of measurements of sensitivity of 100 Ω devices we estimate $\tau_E \simeq 10^{-13}$ seconds. Let us fix the video resistance at a point comparable to the video resistance of a biased point-contact diode, say 1000 Ω. A practical contact radius is 0.1 mil or 2.5 microns. From (37) we find that $\rho = 1$ Ω-cm, corresponding to a carrier density of about 6×10^{15} electrons/cm^3. From (40) we find for the voltage responsivitity $\gamma_0 \simeq 7$ A^{-1}. This is indeed low, compared to the detectors previously discussed, which have $\gamma_0 = \beta_0 R_V$ in the range of 500 to 3000 A^{-1}. Thermoelectric detectors using point contacts can have γ_0 comparable to hot carrier and point-contact diodes, but have extremely high video resistance, in the range of 50 to 100 kΩ. The thermal noise voltage from the device is simply

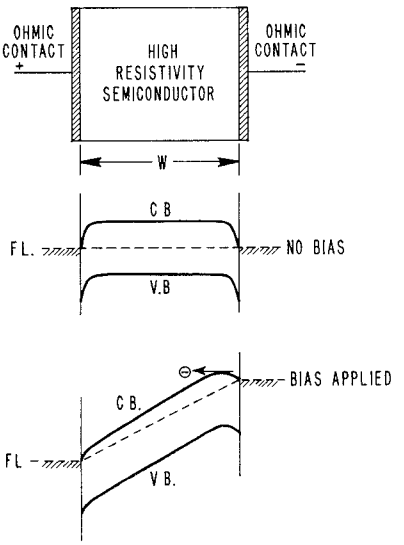

Fig. 9. The space-charge-limited diode (SCLD); device configuration and electronic band diagrams.

$$v_N = \sqrt{4kTR_V} \tag{42}$$

for a video bandwidth of one hertz, or about 4×10^{-9} volts for $R_v = 1000$ Ω. The noise equivalent power NEP can be obtained by writing the equation

$$\gamma_0(\text{NEP}) = v_N \tag{43}$$

and solving for NEP. For the device in question we find NEP $= -62.5$ dBm. Tangential sensitivity is -58.5 dBm, from (2). Referring to (31), notice that for the thermoelectric detector, NEP $= (\text{NEP})_0$; this is equivalent to the statements $f_N \simeq 0$ and $f_c \to \infty$. Applying the criterion equation (13), for the thermoelectric detector, we can calculate the upper square-law limit as -5 dBm. This particular device therefore has a dynamic range of about 53.5 dB, for a 1 Hz video bandwidth. A similar calculation for a 100 Ω device with $\rho \simeq 0.2$ Ω-cm and $r_0 = 2.5\,\mu$ yields TSS $= -50$ dBm and a dynamic range of 54.5 dB. Table I contains this data in summary form with data for the other detectors.

E. The Space-Charge-Limited Dielectric Diode

The space-charge-limited dielectric diode (SCLD) is the solid-state equivalent of the space-charge-limited (SCL) thermionic diode [20]. Space-charge limited flow in insulators and semiconductors is well known, and the analysis of Shockley and Prim [21] is most appropriate for the device as it will be considered here. A fundamental difference in the current transport mechanism in semiconductors gives rise to a square-law component of current in the SCLD, as compared to the corresponding three-halves power component in the SCL thermionic diode. For a semiconductor with a nonnegligible thermal concentration of carriers, e.g., electrons, the

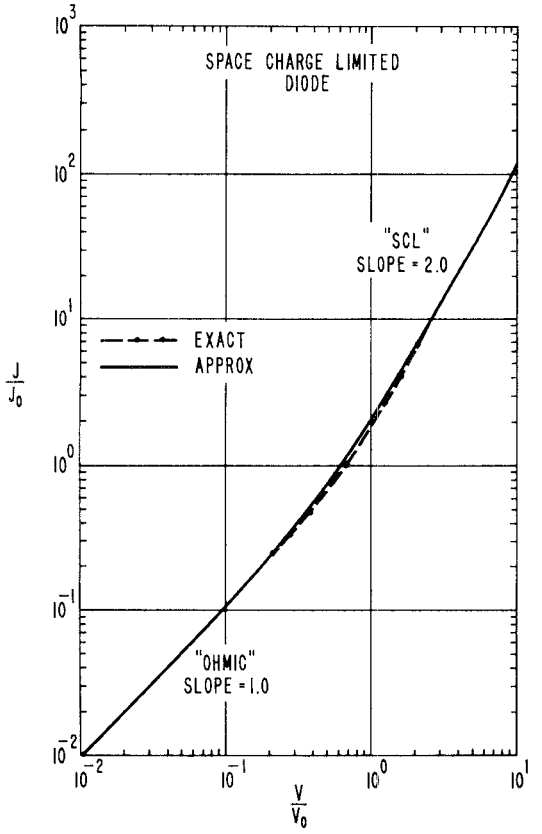

Fig. 10. Exact analysis of Schockley and Prim, and approximate equation (44) in normalized form.

exact analysis of current flow is complicated, but can nevertheless be obtained in parametric form, with electron transit time T as a parameter. If one naïvely proceeded to calculate the current voltage function of the device shown in Fig. 9 by simply superimposing the SCL current upon the low-level (ohmic) current [22], one would obtain the equation

$$J = \frac{q\mu_e n}{W} V + \frac{9}{8} \frac{\mu_e \epsilon}{W^3} V^2 \tag{44}$$

where n is the semiconductor carrier concentration, μ_e the carrier mobility, ϵ the dielectric constant, V the applied voltage, and J the current density. In Fig. 10 the exact analysis of Shockley and Prim and the approximate form (44) are compared in normalized form. The agreement is indeed good. The approximate form for the voltage current function is an adequate engineering approximation, and introduces considerable simplification into the analysis. Referring again to Fig. 10, we observe that for low voltages the "ohmic" or linear current prevails, while at higher voltages, the space-charge-limited (SCL) current begins to dominate. For a semiconductor with higher resistivity (fewer free carriers), the linear region is smaller, and the onset of SCL current occurs at a lower voltage. Fig. 11 shows experimental data from a typical SCLD fabricated in the authors' laboratories: the circles are data points, the

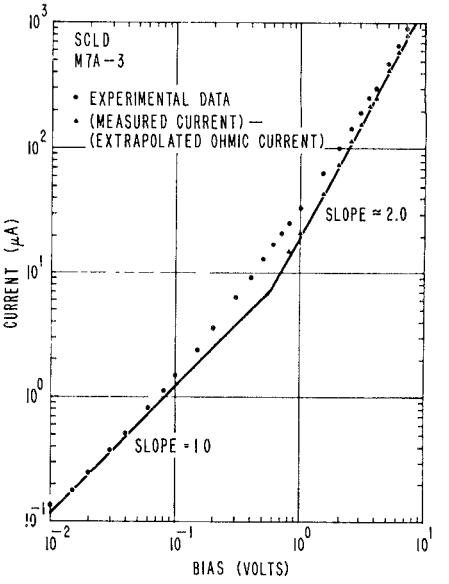

Fig. 11. SCLD i-v characteristic.

triangles are points generated by subtracting the extrapolated linear current from data points, leaving the square-law component.

Nonlinear mobility considerations in the SCLD predict third- and fourth-order terms in the i-v characteristic of the device. If we use the relation [23]

$$\mu_e = \mu_0(1 - \beta E^2) \tag{45}$$

to describe the behavior of the mobility with electric field, we obtain

$$J = k_1 V + k_2 V^2 + k_3 V^3 + k_4 V^4 \tag{46}$$

where the first two terms are in (44), and

$$k_3 \simeq - \frac{\beta}{W^2} k_1 \tag{47}$$

$$k_4 \simeq - \frac{\beta}{W^2} k_2. \tag{48}$$

These are approximate relations, accurate within a factor of less than two, and obtained by simply substituting (45) for μ_e in (44) and approximating E by V/W. For n-type silicon, the coefficient β is about 5×10^{-8} cm^2/volt^2 and for a device 10 microns thick, we have $\beta/W^2 \simeq 0.05$ volt^2.

The noise in SCL devices is expected to be space-charge suppressed, as in the thermionic diode [24], [25]. Van der Ziel [25] suggests that the noise from an SCL device should be much less than the thermal noise appropriate to the dynamic resistance of the device. Unfortunately, no experimental data is available at this time either to verify or contradict existing theories. For lack of such experimental data, we shall conservatively assume that the noise in the device is equal to thermal noise at ambient temperature. This assumption has also been made by Webb and Wright [26].

For low frequencies, the current responsivity of the device, from (8) and (46), is

$$\beta_0 \simeq \frac{1}{2} \frac{2k_2}{k_1 + 2k_2V} \tag{49}$$

where we have neglected terms containing k_3 and k_4. For a device with perfect square-law response, the current responsivity would be

$$\beta_0(\text{perf sq. law}) = \frac{1}{2V} . \tag{50}$$

The dynamic video resistance is

$$R_V = \frac{1}{f^{(1)}} \simeq \frac{1}{(k_1 + k_2V)A} \tag{51}$$

where A is the cross-sectional area, and where we have again neglected k_3 and k_4.

Let us consider a device with area 1.25×10^{-3} cm^2, thickness 10 microns, fabricated from 10 000 Ω-cm n-type silicon, and biased to 0.5 volt. Using (49), (52), (53), and finally (8) and (49), we obtain $\beta_0 \simeq 1.0$ volt^{-1}, and $\Delta \simeq 37\ P_{RF}$. Considering the device as a resistor at thermal equilibrium to calculate noise, as discussed earlier, we can use (51) to calculate R_V, and using the equivalent circuit of Fig. 2, we find $(NEP)_0$ to be -82.5 dBm. Using (13), we find P_{RF}(USL) to be -6 dBm. Tangential sensitivity TSS is -78.5 dBm, and square-law range is 72.5 dB. The video resistance, from (51), is about 500 ohms. The calculated data for this device and for a device with the same area but $W \simeq 25\ \mu$ are shown in Table I.

The RF equivalent circuit for the SCLD has been developed by Shao and Wright [27], who present experimental verification for their theory, using CdS SCL devices. They obtain the equivalent circuit as a parallel conductance and capacitive susceptance; the device has no series resistance as such. In terms of the video resistance R_V, the low frequency conductance and susceptance can be written

$$G_0 = \frac{1}{R_V} \tag{52}$$

$$\beta_0 = \frac{\theta}{4R_V} \tag{53}$$

where $\theta = \omega T$ is the transit angle of the device; T is the electron transit time and ω the radian frequency of the microwave signal. The transit time can be obtained conveniently from the relation

$$T \simeq 3R_VC \tag{54}$$

where C is the geometrical capacitance of the device. For the device considered above, we find $T \simeq 2$ ns.

Shao and Wright find that when $\theta > 0$, the conductance decreases somewhat, and that the susceptance is steadily increasing, roughly as though it were a constant value capacitance. Above $\theta = 2\pi$, the conductance remains relatively constant at about one half its low-frequency value, varying periodically with θ. It has been predicted by Wright [28] that the detected current for a fixed microwave input voltage remains practically constant, at least up to $\theta \simeq 2\pi$. It would therefore appear that this device could be useful as a broadband detector for UHF and microwave frequencies. Its extremely large dynamic range would make it useful in microwave power measuring instrumentation, where accurate square-law response is desired over a wide range.

IV. Summary

A quantitative comparison between two, or among several detectors is appropriate if other factors, e.g., cost and burnout, are either equal or not important. The most important properties which are amenable to quantitative comparison are threshold sensitivity, square-law range, and frequency response. We have obtained a convenient method for comparing devices from a narrow video bandwidth viewpoint, viz. the NEP contour plot method. This method is useful for a detailed quantitative comparison over the entire RF and video frequency spectrum.

The effectiveness of comparison by NEP contours is emphasized in Fig. 12. Here we show the results of increasing bias current in hot carrier and point-contact diodes in order to obtain a better broadband match to a 50 ohm RF source. By comparing these contours with those examined in Figs. 4 and 5, the effects of bias on the contour values and on the shape of the preference boundary are obvious. Notice in particular the change in the shape of the preference boundary.

The thermoelectric detector, since $f_N = 0$ and $f_c \simeq \infty$, has no NEP contours as such. The surface describing NEP for the thermoelectric detector is simply a plane corresponding to $\text{NEP} = (\text{NEP})_0 = \text{constant}$. The thermoelectric detector can be compared with other devices on the (f_V, f_{RF}) plane, and as an example we show in Fig. 12 a 100 Ω thermoelectric detector compared to the hot carrier and point-contact diode. This particular device has very low sensitivity because of its low resistance, and hence has a very small preference region at high radio frequencies. It is superior in this region by virtue of its extremely high cutoff frequency.

Table I shows the comparison of $(NEP)_0$ and dynamic range for typical devices out of the six device classes considered in this paper. We have calculated dynamic range for the case where $f_{RF} \ll f_c$ and $f_V \gg f_N$. In general, we see that increased dynamic range is gained at the expense of threshold sensitivity; the barrier devices are the most sensitive, i.e., tunnel and back diodes, hot carrier and point-contact diodes, but have relatively poor dynamic range. Dynamic range of the HCD or PCD can be improved by biasing to lower video resistances, although the increase in dynamic range is accompanied by a degradation in sensitivity. There is a point beyond which biasing the PCD or HCD ceases to

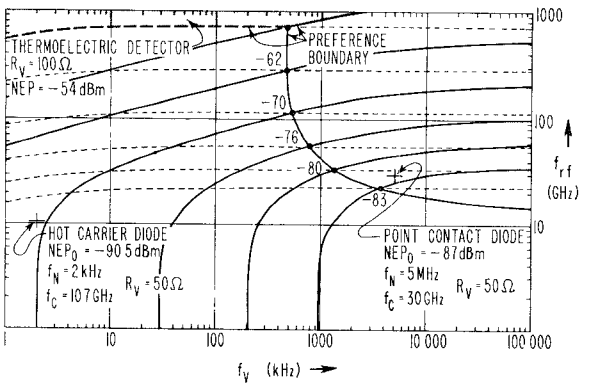

Fig. 12. NEP contours and preference regions for hot carrier and point-contact diode biased to 50 ohms. Also included is a thermoelectric detector with $R_v = 100$ ohms.

improve dynamic range, due to series resistance effects in the diode; it is obviously impossible to bias the device to a video resistance R_V less than R_s. Also, at video frequencies in the $1/f$ noise region, a further decrease in sensitivity is suffered due to an increase of $1/f$ noise with bias.

Dynamic range is larger for the 500 Ω SCLD than for the other devices. This device has somewhat poorer threshold sensitivity than the barrier-type devices, however. The larger dynamic range predicted for this device suggests its potential usefulness in power-monitoring instrumentation.

V. Discussion and Conclusions

Six classes of solid-state microwave detectors have been compared in this paper. The criteria for comparison were sensitivity, frequency response, and dynamic range. To conclude the paper, we now present some general observations regarding each of the six device classes.

The point-contact diode has, as its chief technical advantage over other detectors, an extremely low junction capacitance, resulting from the small-junction area point-contact geometry. Other advantages include a long history of successful use and development in the field of microwave detection and mixing, extending back almost thirty years. From the standpoint of semiconductor technology, the point-contact diode concept is one which has inherent disadvantages. The chief one among these is the fact that fabrication of these devices is accomplished by empirical methods, many of which are still not well understood. Point-contact diodes are, in principle, Schottky barrier devices; however, their i-v characteristics almost never show good agreement with Schottky theory, due mostly to the method of fabrication. The low-frequency noise characteristics present a particularly severe problem where the operation of the devices as video detectors or Doppler mixers is concerned; it is almost certain that the $1/f$ noise results from lack of stability of the semiconductor surface and lack of control over device properties inherent in the manufacturing technique. Indeed, reference to Figs. 4 and 5 clearly shows the superiority of a planar Schottky barrier ("hot carrier") diode in the low video frequency region; this superiority is due entirely to the improvement in $1/f$ noise shown in Fig. 3. Despite its disadvantages, however, it is clear that the ability of the point contact diode to operate well into the millimeter wave region, due to its small capacitance, will assure its existence in the microwave diode field for some years to come, at least until planar techniques have been substantially improved.

The planar Schottky barrier or hot carrier diode is a relative newcomer to the field of microwave detection and mixing. Commercial units are presently available; these have a high degree of uniformity, obey Schottky theory almost perfectly, and have extremely low $1/f$ noise. Because of their uniformity and ideal theoretical performance, they are readily analyzed, and circuits using these devices can be designed theoretically rather than empirically. It seems certain at this time that the planar Schottky barrier diode will eventually replace the point-contact diode in microwave detection and mixing applications; indeed, recent reports [29] indicate that practical hot carrier diodes can, even at this time, be fabricated for frequencies in the 50 GHz range. Chief limiting factor for the planar devices is their barrier capacitance; as planar technology is further developed, this problem is sure to be overcome. Other practical advantages of the planar devices are that they are readily adaptible to low-inductance packaging techniques, and can have better burnout characteristics than the point-contact diodes.

Tunnel diodes, when biased near the peak current, provide better threshold sensitivity than any other device. They are, generally speaking, severely limited by junction capacitance, which results from an extremely narrow junction. Dynamic range of these devices is generally poor, also, due to the sharp nonlinearity of the device near its peak current. Low-frequency noise characteristics appear to be better than for point-contact diodes, but inferior to those of the planar Schottky barrier and back diodes.

Back diodes, identical to tunnel diodes in their concept of operation, are usually designed so that they do not require bias during operation as detectors. In this mode of operation, they have no $1/f$ noise, and current responsivity comparable to that of point-contact and hot carrier diodes. Since series resistance can be made low, the devices have good high-frequency response despite a high barrier capacitance. It would appear that this device, along with the hot carrier diode, will offer serious competition to the point-contact diode in the area of microwave video detection and mixing. A possible disadvantage, as for the tunnel diode, is its susceptibility to accidental burnout, stemming from its extremely low zero-bias resistance.

The thermoelectric detector offers promise of high sensitivity video detection at millimeter wavelengths. Its inherent advantages are almost complete absence of a cutoff frequency, and absence of $1/f$ noise. A serious

disadvantage is the fact that high sensitivity in these devices is always obtained at the expense of extremely high video and RF resistance, typically in the range of 100 kΩ. This implies inherently narrow-band operation in the RF circuit, and poor pulse fidelity, or equivalently, poor bandwidth in the video frequency circuit. Square-law range is also limited by nonlinear mobility effects. Burnout studies reported by Harrison and Zucker [19] indicate that the burnout resistance of these devices is superior to that of conventional silicon point-contact diodes.

The space-charge-limited dielectric diode is probably the least familiar of the six devices discussed in this paper. It is also a device which has received relatively little attention in the literature, either experimentally or theoretically. From the recent work which has been done, as particularly exemplified by the work of Wright, it would seem that the device has promise as a microwave detector and mixer. From the calculations presented in this paper, it is seen that the device can have the advantages of convenient video impedance (e.g., 500 Ω), moderate sensitivity, in addition to a very large range of square-law operation. The frequency response of the device is perhaps in question since no experimental data has been reported for frequencies more than a few times the reciprocal of the transit time. Due to its large-area planar construction, it is also anticipated that this device will have extremely high burnout resistance.

Acknowledgment

The authors would like to express their appreciation to S. Krakauer for suggesting that this work be undertaken, and for numerous stimulating discussions during its course. Discussions with W. Grove, R. D. Hall, J. Lepoff, and J. L. Moll were also very helpful, and are gratefully acknowledged.

References

[1] G. U. Sorger and B. O. Weinschel, "Comparison of deviations from square-law for RF crystal diodes and barretters," *IRE Trans. on Instrumentation*, vol I-8, pp. 103–111, December 1959.
[2] H. C. Torrey and C. A. Whitmer, *Crystal Rectifiers*. vol. 15, M.I.T. Rad. Laboratory Ser. New York: McGraw-Hill, 1948.
[3] K. Ishii and A. L. Brault, "Noise output and noise figure of biased millimeter-wave detector diodes," *IRE Trans. on Microwave Theory and Techniques*, vol. MTT-10, pp. 258–262, July 1962.
[4] B. G. Bosch et al., "Excess noise in microwave mixer crystals," *Proc. IRE* (*Correspondence*), vol. 49, pp. 1226–1227, July 1961.
[5] G. R. Nicoll, "Noise in silicon microwave diodes," *Proc. IEE* (*London*), vol. 101, pt. 3, pp. 317–324, September 1964.
[6] A. Uhlir, Jr., "Characterization of crystal diodes for low-level microwave detection," *Microwave J.*, vol. 6, pp. 59–67, July 1963.
[7] A. Van der Ziel and A. G. T. Becking "Theory of junction diode and junction transistor noise," *Proc. IRE*, vol. 46, pp. 589–594, March 1958.
[8] H. O. Sorensen, "Using the hot carrier diode as a detector," *Hewlett-Packard J.*, vol. 17, pp. 2–5, December 1965.
[9] L. Esaki, "New phenomenon in narrow germanium p-n junctions," *Phys. Rev.*, vol. 109, pp. 603–604, 1958.
[10] P. E. Chase and K. K. N. Chang, "Tunnel diodes as millimeter wave detectors and mixers," *IRE Trans. on Microwave Theory and Techniques* (*Correspondence*), vol. MTT-11, pp. 560–561, November 1963.
[11] M. D. Montgomery, "The tunnel diode as a highly sensitive microwave detector," *Proc. IRE* (*Correspondence*), vol. 49, pp. 826–827, April 1961.
[12] C. A. Burrus, Jr., "Backward diodes for low-level millimeter-wave detection," *IEEE Trans. on Microwave Theory and Techniques*, vol. MTT-11, pp. 357–362, September 1963.
[13] T. P. Brody and P. H. Boyer, "Evaluation of Esaki integrals and approximation of tunnel diode characteristics," *Solid-State Electronics*, vol. 2, pp. 209–215, May 1961.
[14] C. W. Bates, "Tunneling currents in Esaki diodes," *Phys. Rev.*, vol. 121, p. 1071, 1961.
[15] S. T. Eng, "Low-noise properties of microwave backward diodes," *IRE Trans. on Microwave Theory and Techniques*, vol. MTT-9, pp. 419–425, September 1961.
[16] R. B. Mouw and F. M. Schumacher, "Tunnel diode detectors," *Microwave J.*, vol. 9, pp. 27–36, January 1966.
[17] T. Yajima and L. Esaki, "Excess noise in narrow germanium p-n junctions," *J. Phys. Soc.* (*Japan*), vol. 13, pp. 1281–1287, November 1958.
[18] W. C. Follmer, "Low-frequency noise in backward diodes," *Proc. IRE* (*Correspondence*), vol. 49, pp. 1939–1940, December 1961.
[19] R. I. Harrison and J. Zucker, "Hot-carrier microwave detector," *Proc. IEEE*, vol. 54, pp. 588–595, April 1966.
[20] G. T. Wright, "Mechanisms of space-charge-limited current in solids," *Solid-State Electronics*, vol. 2, pp. 165–189, 1961.
[21] W. Shockley and R. C. Prim, "Space-charge limited emission in semiconductors," *Phys. Rev.*, vol. 90, pp. 753–758, June 1, 1953.
[22] M. A. Lampert, "Injection currents in insulators," *Proc. IRE*, vol. 50, pp. 1781–1796, August 1962.
[23] M. A. C. S. Brown, "Deviations from Ohm's law in germanium and silicon," *J. Phys. Chem. Solids*, vol. 19, pp. 218–227, May 1961.
[24] V. Sergiescu, "Space-charge reduction of shot noise for space-charge-limited current in solids," *Brit. J. Appl. Phys.*, vol. 16, pp. 1435–1447, October 1965.
[25] A. Van der Ziel, "Low frequency noise suppression in space-charge-limited solid-state diodes," *Solid-State Electronics*, vol. 9, pp. 123–127, February 1966.
[26] P. W. Webb and T. T. Wright, "Dielectric triode: A low-noise solid-state amplifier," *J. Brit. IRE*, vol. 23, pp. 111–113, February 1962.
[27] J. Shao and G. T. Wright, "Characteristics of the space-charge limited diode at very high frequencies," *Solid-State Electronics*, vol. 3, pp. 291–303, November/December 1961.
[28] G. T. Wright, "Transit time effects in the space-charge-limited silicon microwave diode," *Solid-State Electronics*, vol. 9, pp. 1–6, January 1966.
[29] D. T. Young and J. C. Irvin, "Millimeter frequency conversion using Au-n-type GaAs Schottky barrier epitaxial diodes with a novel contacting technique," *Proc. IEEE* (*Correspondence*), vol. 53, pp. 2130–2131, December 1965.